Journal of ELECTRONIC MATERIALS, Vol. 47, No. 5, 2018
https://doi.org/10.1007/s11664-018-6138-4

Second-Order Magnetic Transition and Low Field Magnetocaloric Effect in Nanocrystalline Pr_5Co_{19} Compound

W. BOUZIDI,[1,2,3] N. MLIKI,[2] and L. BESSAIS[1]

1.—Université Paris Est, ICMPE, (UMR7182), CNRS-UPEC, 94320 Thiais, France. 2.—Laboratoire Matériaux Organisation et Propriétés (LR99ES17), Faculté des Sciences de Tunis, Université de Tunis El Manar, 2092 Tunis, Tunisia. 3.—e-mail: bouzidi@icmpe.cnrs.fr

Magnetic and magnetocaloric properties have been studied for the Pr_5Co_{19} compound crystallized in the Ce_5Co_{19}-type structure (space group $R\bar{3}m$). We report a large magnetic entropy change ($-\triangle S_M^{max}$) at Curie temperature, using the thermodynamic Maxwell's relation, which reaches a maximum of 5.2 J/(kg K) under a low magnetic field of 0-1.5 T. The temperature dependence of the magnetization and the Arott plots around the second order magnetic transition for this compound are also reported. The temperature dependence of the Landau coefficients has been derived by fitting the magnetization, using the Landau expansion of the magnetic free energy.

Key words: Intermetallics, nanomaterials, magnetocaloric effect, x-ray-diffraction, Magnetism

INTRODUCTION

Rare earth (R) and transition metal (T) based intermetallics have become well-known mainly as hard magnetic materials. They give rise to a great variety of functional materials for technological applications[1] such as permanent magnets, semi-hard or soft magnetic materials as well as for magnetic refrigeration.[2] The latter application is based on the magnetocaloric effect (MCE), an intrinsic property of magnetic materials. Compared with the conventional refrigeration technology based on gas compression and expansion, magnetic refrigeration is advantageous as an environmentally friendly and energy-saving technology.[3,4] It is also a silent cooling technique because of the absence of compressor.

The study of the MCE was basically explored by Weiss and Piccard when studying the magnetic behaviors of iron.[5] MCE is based on the fact that at a fixed temperature, following the application of a magnetic field, the entropy of a system of magnetic moments can be reduced. Entropy is a measure of the disorder in such a system, so the entropy increases when the disorder is higher. Under a magnetic field, the moments will become partly aligned, which means that the magnetic field decreases the entropy. The magnetocaloric effect also becomes lower if the temperature is lowered because the moments become more aligned. One of the first studies of systems exhibiting a giant magnetocaloric effect was based on $Gd_5(Ge,Si)_4$ compounds.[6] Other studies show large magnetic entropy changes at low Curie temperature ($\triangle S = 24.4\,J/(kg\,K)$ at $T_C = 200.2\,K, H = 2\,T$ and $\triangle S = 5.37\,J/(kg\,K)$ at $T_C = 29\,K, H = 5\,T$), respectively, of $LaFe_{11.6}Si_{1.4}$ and $SmNi_5$ compounds.[7,8]

The search for the best prototypes for high temperature magnetic refrigeration are mainly focused in rare-earth based materials, due to their important magnetic characteristics and considering that they are energetically very attractive.[9,10] The Pr_5Co_{19} compound can be obtained by stacking hexagonal structure cells of $PrCo_5$ ($CaCu_5$-type structure) and cubic cells of $PrCo_2$ ($MgCu_2$-type structure) along a common hexagonal. The Pr_5Co_{19} compound has a structure with more cells than Pr_2Co_7[11] and $PrCo_3$.[12]

In the search for new compounds presenting high magnetocaloric effects, we have synthesized the nanocrystalline transition metal rich Pr_5Co_{19}. Here,

(Received June 23, 2017; accepted February 9, 2018; published online February 22, 2018)

we study the magnetic properties and magnetocaloric effect of this compound.

EXPERIMENT

The Pr_5Co_{19} compound was prepared by arc melting in a water-cooled copper hearth with an unconsumable tungsten electrode under a purified argon atmosphere. An excess of praseodymium powder was used in order to maintain an over-pressure of Pr on the sample. Milling was performed for 5h with ball to powder of 15/1 in a high-energy ball mill.[13] After synthesis, the powder was wrapped into tantalum foil and annealed for 30 min sealed in a silica tube under 10^{-6} Torr at 1048 K.

The phase analysis was performed using x-ray powder diffraction (XRD) on a Bruker D8 diffractometer. The wavelength used was the average wavelength of $K_\alpha 1$ and $K_\alpha 2$, with data collected by 0.015° step width for 13.5 s over a 2θ range and analyzed by the Rietveld method.[14–17] The line shape of the diffraction peaks was generated by a pseudo-Voigt function. The background was shown by interpolation between selected points in regions devoid of Bragg reflections. In the final run, the following parameters were refined: zero point, scale factors U, V, W, unit cell parameters, background points, positional parameters, isotopic thermal factors and preferred orientation parameters.

In order to confirm the composition of the prepared sample, we used the electron dispersive x-ray spectroscopy (EDS) using the transmission electron microscope Tecnai G2 operating at 200 kV, with a LaB_6 source. Measurements of the magnetic and magnetocaloric properties were carried out using differential magnetometer DSM-8 MANICS with a field up to 1.5 T.

RESULTS AND DISCUSSION

Structure Analysis

In order to refine the XRD patterns, it is important to recall that R_5T_{19} compounds crystallize in two different polymorphic forms, the hexagonal Sm_5Co_{19}-type structure[18] (space group $P6_3/mmc$) and the rhombohedral Ce_5Co_{19}-type. However, in our case, whatever the temperature of annealing, the intermetallic Pr_5Co_{19} compound crystallizes in the rhombohedral (space group $R\bar{3}m$). This can be obtained by stacking the hexagonal structure cells of $PrCo_5$ ($CaCu_5$-type structure) and the cubic cells of $PrCo_2$ ($MgCu_2$-type structure) along the common hexagonal axis (Fig. 1). It shows that the unit cell for the rhombohedral structure contains two inequivalent crystallographic sites, one for Pr at 6c and another one at 3a. The Co atoms occupy three crystallographic sites, 6c, 18h and 3b. From the Rietveld refinement, we have deduced the following unit cell parameters: $a = 5.0672(4)$ Å $c = 48.755(4)$ Å and $c/a = 9.622$ Table I. In our system, the unit cell parameter c is greater than the one found for a hard magnetic Pr_2Co_7 compound ($c = 36.549$ Å).[11] As a consequence, we can consider that Pr_5Co_{19} presents a higher uniaxial magnetocrystalline anisotropy. The high coercivity 15 kOe, obtained at room temperature is attributed to the uniaxial anisotropy and to the optimized microstructure developed by the mechanical milling process and subsequent annealing.

Figure 2 shows the XRD pattern of Pr_5Co_{19} samples annealed at 1048 K. All peaks are indexed and confirm the stability of thePr_5Co_{19} phase. The composition of the chemical elements (at.%: Co, Pr) was analyzed using the EDS measurement shown in Fig. 3. A semi quantitative study of the spectrum

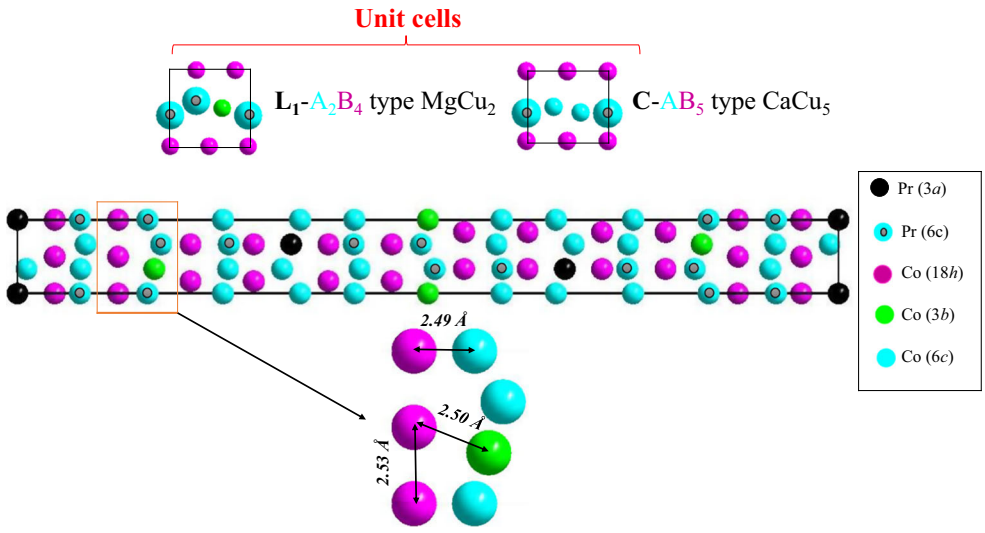

Fig. 1. Crystal structure of Pr_5Co_{19} compound and distance of Co-Co (Color figure online).

Table I. Unit cell parameters *a*, *c*, *c*/*a*, and V, compositions at.% (Co, Pr) of Pr_5Co_{19} (Annealed at T = 1048 K)

a (Å)	*c* (Å)	*c* / *a*	V(Å)^3	at.% Pr	at.% Co
5.0672 (4)	48.755 (4)	9.622	1084.14	21.8	78.2

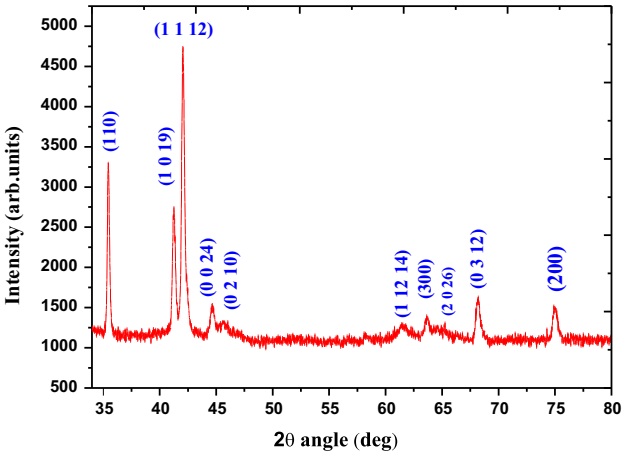

Fig. 2. X-ray diagram patterns of Pr_5Co_{19} compound annealed at 1048 K.

confirms that at.% Pr = 21.8 and for Co is equal to 78.2%. This result is in good agreement with experimental data of synthesis and the Rietveld refinement. The small amount of Cu in the spectrum might be due to the sample carrier being made of copper. The lattice parameters and the compositions of Co and Pr elements are given in Table I.

Magnetic Properties

The temperature dependency of the magnetization shows that $T_c = 690$ K.[19] This paramagnetic–ferromagnetic transition is due essentially to the predominance of the positive Co-Co exchange interactions 3*d*-3*d*.[20,21] It is noteworthy that the interactions between the rare earth and metal transition 3*d*-4*f* are assumed to be weak in comparison with the exchange interactions 3*d*-3*d*. The Curie temperature T_c of Pr_5Co_{19} could be determined by the Co-Co interaction from the following equation (R: Pr; M: Co):[22]

$$T_c = (T_R + T_M + ((T_M - T_R)^2 + 4T_{RM})^{1/2})/2$$

where

$$T_{RM} = (2Z_{RM}(Z_{RM}.Z_{MR}.G_R.G_M))^{1/2},$$

Let's notice that: $T_{ii} = (2A_{ii}.Z_{ii}.G_i)/(3k_B)$, $(i = \mathrm{R}, \mathrm{M})$, with G_i as the de Gennes factor.

In order to analyze the nature of the magnetic transition and consequently the magnetocaloric effect, we measured the magnetization isotherms at various temperatures from 672 K to 708 K with steps of 3 K. The resulting curves are presented in Fig. 4.

According to the spin fluctuation model based on the Landau theory,[23,24] the magnetic free energy $F(M, T)$, can be generally expressed as follows:

$$F = \frac{1}{2}a(T).M^2 + \frac{1}{4}b(T).M^4 + \frac{1}{6}c(T).M^6 + \cdots - \mu_0 H \quad (1)$$

The nature of the magnetic transition (first/second order phase transition) was determined by the temperature and magnetic field dependencies. The $a(T)$, $b(T)$, and $c(T)$ coefficients represent a temperature dependency according to the thermal variation of amplitude of spin fluctuation. We used the thermal equilibrium conditions $(\mathrm{d}F/\mathrm{d}M = 0)$ to determine the total magnetization around the Curie temperature:

$$\mu_0 H = a(T) + b(T).M^3 + c(T).M^5 \quad (2)$$

From Eq. (2), $a(T)$, which is always positive, permits us to obtain the value of the Curie temperature. On the other hand, the order of magnetic transition depends on the sign of $b(T)$ at the transition. The magnetic transition is of first order when the Landau parameter $b(T)$ is negative $(b(T_c) < 0)$. When $b(T_c)$ is positive $(b(T_c) > 0)$, the transition is of second order. Note that $c(T_c)$ is always positive.[25] Figure 5 shows the evolution of the Landau parameters $a(T)$, $b(T)$, and $c(T)$ as a function of temperature for Pr_5Co_{19} compound. As predicted, the magnetic transition is of second order, given that $b(T)$ is eventually positive after T_c.

Analysis of Arott's plots, M^2 versus H / M, obtained from the magnetic field dependency of isothermal magnetization, is shown in Fig. 6. The positive slope and linear behavior near T_c confirm that the magnetic phase transition is of second order from the ferromagnetic to the paramagnetic state.

Magnetocaloric Effect

The magnetocaloric effect has been calculated in terms of isothermal magnetic entropy change $\triangle S_M$

$$\text{where} \begin{cases} G_i = (g_i - 1)^2 J_i(J_i + 1),\ g_i \text{ is the Lande factor of the } i \text{ atom} \\ Z_{ij} : \text{the number of nearest } j \text{ neighbor atom of an } i \text{ atom} \end{cases}$$

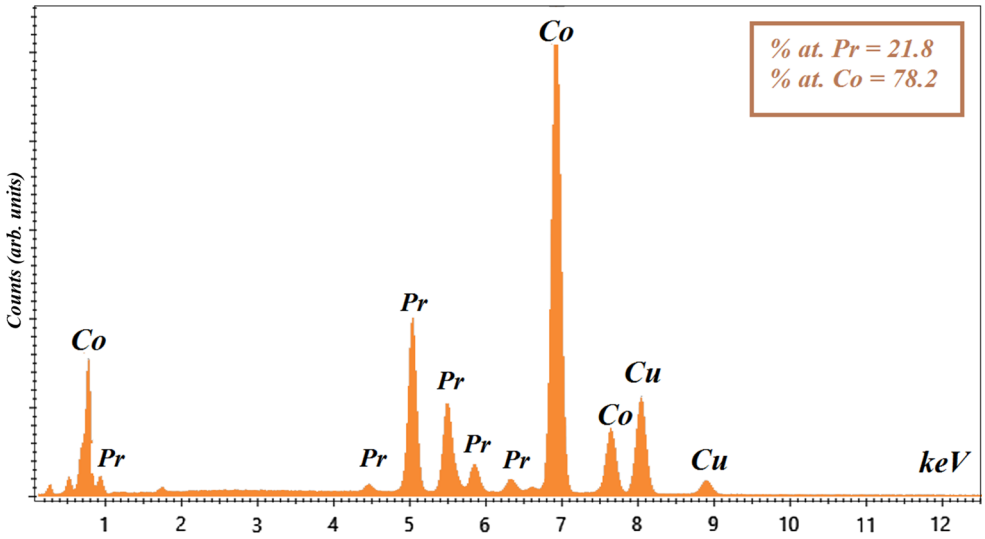

Fig. 3. EDS spectrum of Pr_5Co_{19} compound.

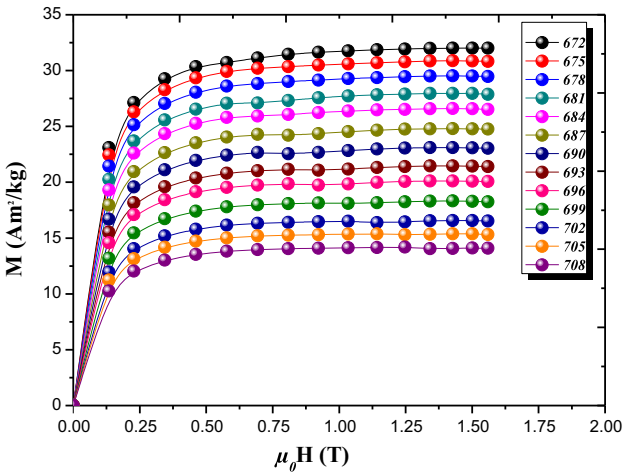

Fig. 4. Isotherm magnetization curves, M(H), for Pr_5Co_{19} compound (Color figure online).

using magnetization isotherms obtained at different temperatures. $M(H)$ measured at various temperatures from 672 K to 708 K with steps of 3 K are represented in Fig. 4. Magnetic entropy change was determined as a function of temperature T and the applied magnetic field H based on Maxwell's thermodynamic relations. It is given by the following equation:[26,27]

$$\triangle S_M(T,\triangle H) = S_M(T,H) - S_M(T,0) = \int_0^{\mu_0 H_{\max}} \left(\frac{\partial S(T,H)}{\partial H}\right)_T dH \quad (3)$$

From Maxwell's thermodynamic relation

$$\left(\frac{\partial S(T,H)}{\partial H}\right)_T = \left(\frac{\partial M(T,H)}{\partial T}\right)_H \quad (4)$$

Finally, we can obtain the equation of magnetic entropy variation:

$$\triangle S_M(T,\triangle H)_{\triangle H} = \int_0^{\mu_0 H_{\max}} \left(\frac{\partial M(T,H)}{\partial T}\right)_H dH \quad (5)$$

Also, the magnetocaloric effect can be calculated indirectly from the magnetization isotherm data using the numerical integration:

$$\triangle S_M(T_i,\triangle H) = \mu_0 \sum_i \frac{M_{i+1} - M_i}{T_{i+1} - T_i} \triangle H_i \quad (6)$$

where μ_0 is the vacuum magnetic permeability, M_i and M_{i+1} are the magnetization values measured at T_i and T_{i+1} in a field change of $\triangle H_i$.[28]

From these calculations, we deduce that there is an evolution of $\triangle S_M$ with temperature and applied field. Fig. 7 illustrates the thermal variation of magnetic entropy change for the Pr_5Co_{19} compound. The $(-\triangle S_M^{\max})$ is found to increase with increasing temperature reaching a maximum value at T_c. It can be seen from Fig. 7 that the maximum value is around 5.2 J/(kg K) under a magnetic field of 0-1.5 T. In fact, there are two major contributions to the maximum change of magnetic entropy $\triangle S_M$: the saturation magnetization M_S and $\triangle M_T(H)$, which is the difference between two consecutive isotherms at a given magnetic field around the transition temperature.

It is important to note that the $\triangle S_M$ of Pr_5Co_{19} is significant compared to other commonly researched magnetic refrigerant materials, such as $Pr_2Fe_{17}(\triangle S = 2\,J/(kg\,K),\ \mu_0 H = 1.5\,T)$,[29] $SmNi_5$ $(\triangle S = 1.2\,J/(kg\,K),$[8] $\mu_0 H = 1.5\,T)$ and $GdNi_3FeSi$ $(\triangle S = 0.5\,J/(kg\,K),\ \mu_0 H = 1.5\,T)$.[30] $(-\triangle S_M^{\max})$, Curie temperature and applied field are shown in Table II. The second parameter characterizing the magnetocaloric effect is the relative cooling power (RCP),

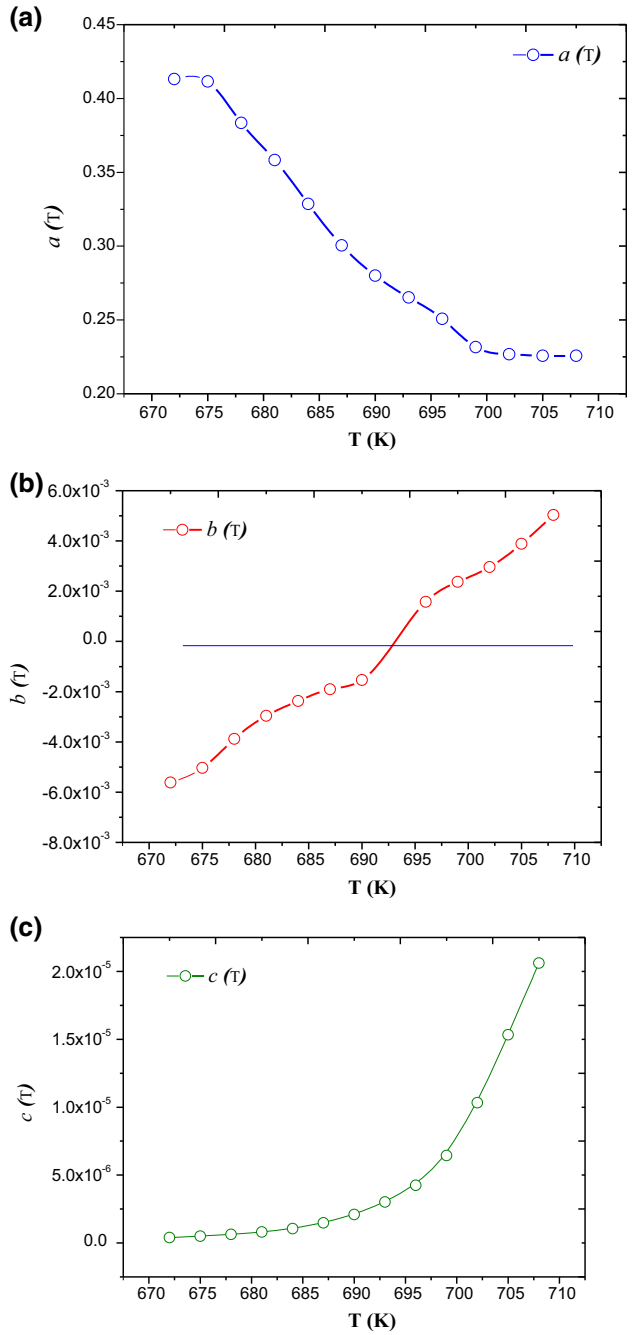

Fig. 5. Temperature dependency of Landau coefficients for Pr_5Co_{19} compound, (a) Landau coefficient $a(T)$, (b) Landau coefficient $b(T)$, and (c) Landau coefficient $c(T)$.

which is equal to 18.2 J/kg for Pr_5Co_{19} compound, compared with 4.8 J/kg for $SmNi_5$.[8] Its determination is based on the magnetic entropy change,[31,32] according to the following formula:

$$\mathrm{RCP} = -\triangle S_M \delta T_{FWHM} \qquad (7)$$

where $\triangle S_M$ and δT_{FWHM} are the maximum of the entropy variation and the full-width at half-

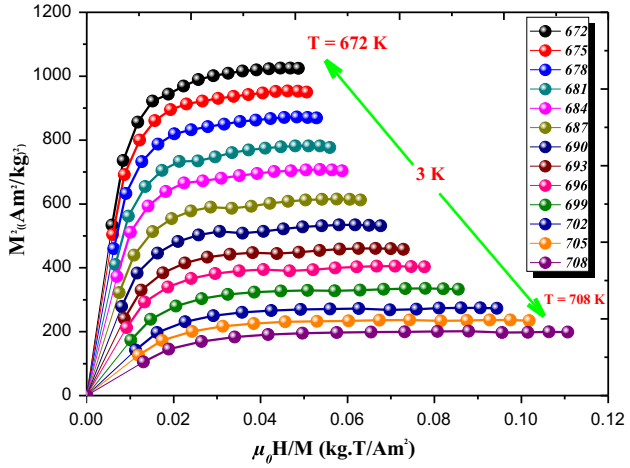

Fig. 6. The Arrott plots of Pr_5Co_{19} compound (Color figure online).

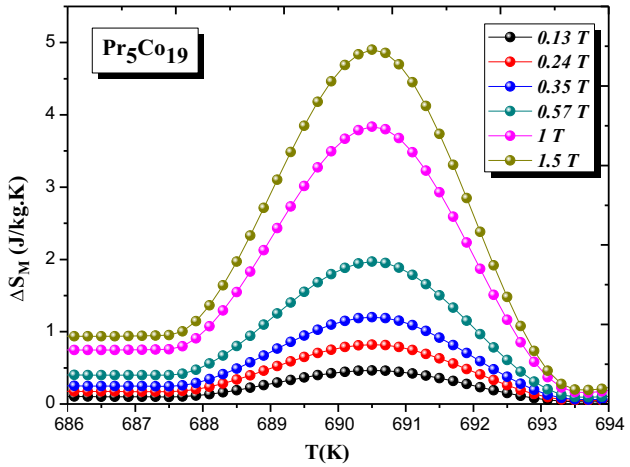

Fig. 7. Magnetic entropy change $\triangle S_M$ versus temperature around the Curie temperature for Pr_5Co_{19} compound (Color figure online).

Table II. Summary of magnetocaloric properties of Pr_5Co_{19} compound compared with other magnetic materials

Compound	$\mu_0 H$ (T)	T_c (K)	$-\triangle S_M^{max}$ J/(kg K)	Ref.
Pr_5Co_{19}	1.5	690	5.2	This work
$Gd_2Fe_{16}Si$	1.5	522	3.07	33
$Nd_2Fe_{15}Co_2$	1.5	563	5.83	34
Pr_2Co_7	1.5	580	3.8	35
Gd	1.5	293	3.8	36
Pr_2Fe_{17}	1.5	285	2	29
$SmNi_5$	1.5	29	1.2	8
SmNi	1.5	42	0.65	37
$GdNi_3FeSi$	1.5	168	0.5	30
GdNi	2	69	8.9	38
TbNi	2	67	11.5	38
DyNi	1.5	61	2	39

maximum in the temperature dependency of the magnetic entropy change $\triangle S_M$.[8]

CONCLUSION

In summary, we have studied the magnetic and magnetocaloric properties of Pr_5Co_{19} compound, synthesized by mechanical milling and subsequent annealing. The present study illustrates that the ferromagnetically and hard magnetic Praseodymium-based 5:19 compound shows a second order magnetic phase transition in the Ce_5Co_{19}-type structure with $R\bar{3}m$ space group. The nanocrystalline magnet Pr_5Co_{19} , based on rare earth and transition metals, presents a good magnetocaloric effect with ($-\triangle S_M^{\max}$ = 5.2 J/(kg K)) under a low magnetic field of 0-1.5 T. These results indicate that the compound is an attractive alloy due to its good intrinsic magnetic properties, suitable not only for permanent magnet applications, but also, and mostly, for magnetic refrigeration at high temperatures (heat pump).

ACKNOWLEDGEMENTS

This work was supported by the National Center for Scientific Research (CNRS), France, the "Ministère de l'Enseignement Supérieur et de la Recherche Scientifique" (LR99ES17) and by PHC-MAGHREB Project 15/MAG07.

REFERENCES

1. K. H. J. Buschow, *Rep. Prog. Phys.* 40, 1179 (1977).
2. V. K. Pecharsky, K. A. Gschneidner, A. O. Pecharsky, and A. M. Tishin, *Phys. Rev. B* 64, 144406 (2001).
3. A. Kitanovski and P.W. Egolf, *Int. J. Refrg* 38, 449 (2010).
4. M. Rosca, M. Balli, D. Fruchart, D. Gignoux, E.K. Hlil, S. Miraglia, B. Ouladdiaf, and P. Wolfers, *J. Alloys Compd.* 50, 490 (2010).
5. P. Weiss and A. Piccard, *C. R. Hebd. Acad* 166, 352 (1918).
6. V. K. Pecharsky and K. A. Gschneidner, *Phys. Rev. Lett.* 78, 4494 (1997).
7. M. Phejar, V. Paul-Bancour, and L. Bessais, *Intermetallics* 18, 2301 (2010).
8. K. Nouri, M. Jemmali, S. Walha, K. Zehani, A. B. Sala, and L. Bessais, *J. Alloys Compd.* 672, 440 (2016).
9. K. Gschneidner Jr, V. Pecharsky, and A. Tsokol, Reports on Progress in Physics *68*, 1479 (2005).
10. A.M. Tishin, Y.I. Spichkin, *The Magnetocaloric Effect and Its Applications* (Bristol, 2003).
11. R. Fersi, N. Mliki, L. Bessais, R. Guetari, V. Russier, and M. Cabié, *J. Alloys Compd.* 522, 14 (2012).
12. K. Younsi, V. Russier, and L. Bessais, *J. Appl. Phys.* 107,8 (2010).
13. L. Bessais, E. Dorolti, and C. Djega-Mariadassou, *J. Appl. Phys*. 97, 013902 (2005).
14. H. Rietveld, *Acta Crystallogr*. 22, 151 (1967).
15. H. Rietveld, *Acta Crystallogr.* 2, 65 (1969).
16. J. Rodrguez-Carvajal, *Physica B* 192, 55 (1993).
17. L. Bessais, K. Younsi, S. Khazzan, and N. Mliki, *Intermetallics* 19, 997 (2011).
18. Y. Khan, *Acta Crystallogr*. 30, 1533 (1974).
19. W. Bouzidi, N. Mliki, and L. Bessais, *J. Magn. Magn. Mater.* 441, 566 (2017).
20. E. Belorizky, M. Fremy, J. Gavigan, D. Givord, H.S. Li, *J. Appl. Phys*. 61, 3971 (1987).
21. J. Franse, R. Radwanski, Handbook of Magnetic Materials (Elsevier, Amsterdam, 1993).
22. Y. Chen, X. Liang, and L. Chen, *Phys. Rev. B* 61, 5 (2000).
23. J. Inoue and M. Shimizu, *J. Phys. F* 12, 1811 (1982).
24. P. E. Brommer, *Physica B* 154, 197 (1989).
25. R. Guetari, T. Bartoli, C. Cizmas, N. Mliki, and L. Bessais, *J. Alloys Compd.* 684, 291 (2016).
26. V. K. Pecharsky and K. A. Gschneidner, *J. Appl. Phys.* 86, 565 (1999).
27. F. Hu, B. Shen, J. Sun, Z. Cheng, X. Zhang, *J. Phys. Condens. Matter* 12:L691, 6 (2000).
28. M. Foldeaki, R. Chahine, and T. Bose, *J. Appl. Phys*. 77, 3528 (1995).
29. K. Zehani, R. Guetari, N. Mliki, and L. Bessais, *Int. Conf. Magn.* 75, 1435 (2015).
30. A.V.Morozkin, A.V.Knotko, V.O.Yapaskurt, J. Yao, F.Yuan, Y.Mozharivskyj, R. Nirmala, S.Quezado, and S.K.Malik, *J. Solid State Chem.* 232, 150 (2015).
31. D. K. Anh, N. Thuy, N. Duc, T. Nhien, and N. Nong, *J. Magn. Magn. Mater.* 262, 427 (2003).
32. M. Balli, M. Rosca, D. Fruchart, and D. Gignoux, *J. Magn. Magn. Mater.* 321, 123 (2009).
33. K. Nouri, T. Bartoli, A. Chrobak, L. Bessais to be published (2017).
34. N. Bouchaala, M. Jemmali, T. Bartoli, K. Nouri, I. Hentech, S. Walha, L. Bessais, A.B. Salah, to be published (2017).
35. R. Fersi, W. Bouzidi, N. Mliki, L. Bessais, to be published (2017).
36. J. Shen, J.-F. Wu, and J.-R. Sun, *J. Appl. Phys*. 106, 083902 (2009).
37. H. Drulis, A. Hackemer, A. Zaleski, Yu.L. Yaropolov, S.A. Nikitin, and V.N. Verbetsky, *Solid State Commun.* 151, 1240 (2011).
38. R. Rajivgandhi, J. A. Chelvane, S. Quezado, S. Malik, and R. Nirmala, *J. Magn. Magn. Mater.* 433, 169 (2017).
39. R. Rajivgandhi, J. AroutChelvane, A.K. Nigam, Je-GeunPark, S.K. Malik, and R. Nirmala, *J. Magn. Magn. Mater.* 418, 9 (2016).